

MARS: Harmonizing Multimodal Convergence via Adaptive Rank Search

Minkyung Cho¹ Insu Jang¹ Shuwei Jin¹ Zesen Zhao¹ Adityan Jothi²
 Ethem F. Can² Min-Hung Chen^{†2} Z. Morley Mao^{†1}

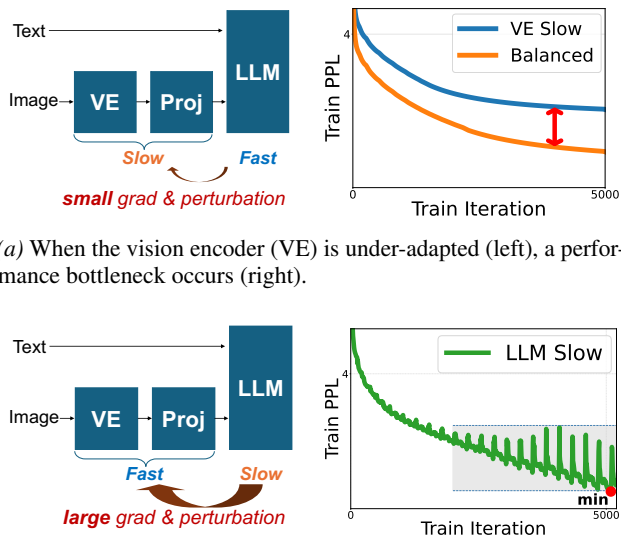
Abstract

Fine-tuning Multimodal Large Language Models (MLLMs) with parameter-efficient methods like Low-Rank Adaptation (LoRA) is crucial for task adaptation. However, imbalanced training dynamics across modalities often lead to suboptimal accuracy due to negative interference, a challenge typically addressed with inefficient heuristic methods such as manually tuning separate learning rates. To overcome this, we introduce **MARS** (Multimodal Adaptive Rank Search), an approach to discover optimal rank pairs that balance training dynamics while maximizing performance. Our key innovation, a proposed framework of dual scaling laws, enables this search: one law models module-specific convergence time to prune the search space to candidates with aligned dynamics, while the other predicts final task performance to select the optimal pair from the pruned set. By re-purposing the LoRA rank as a controller for modality-specific convergence speed, MARS outperforms baseline methods and provides a robust, automated strategy for optimizing MLLM fine-tuning.

1. Introduction

A prominent trend in modern Multimodal Large Language Model (MLLM) research is the shift toward comprehensive fine-tuning of all major components—including the vision encoder (VE), projector, and LLM backbone—to achieve state-of-the-art performance (Zhang et al., 2024b; Zhai et al., 2024; Zanella & Ben Ayed, 2024; Chen et al., 2025). This paradigm shift stems from the growing recognition that simply connecting a vision encoder to a pre-trained LLM is insufficient for unlocking deeply integrated multimodal understanding (Kim et al., 2024). Given the immense scale of these models, this comprehensive adaptation is commonly enabled by parameter-efficient fine-tuning methods like low-

[†] Equal advising. ¹University of Michigan ²NVIDIA. Correspondence to: Minkyung Cho <minkycho@umich.edu>.



(a) When the vision encoder (VE) is under-adapted (left), a performance bottleneck occurs (right).

(b) When the LLM is under-adapted (left), it causes training oscillations (right).

Figure 1. Motivation: Imbalanced training dynamics lead to suboptimal performance. Conceptual cases of module imbalance (left) and their corresponding empirical results (right).

rank adaptation (LoRA) (Hu et al., 2022).

While applying a uniform LoRA rank is common practice, this approach overlooks the distinct learning requirements of each modality and fails to address the critical issue of imbalanced training dynamics, where modules converge at different rates. As illustrated in Figure 1, this imbalance can lead to performance bottlenecks and training oscillations. A common alternative, heuristically tuning differential learning rates, is often laborious and relies on costly trial-and-error experimentation (Li et al., 2024; Bai et al., 2025; Zhang et al., 2024b). Given the learning rate only controls the speed of learning via gradient scaling, a more fundamental strategy is to adjust the LoRA rank, which directly controls a module’s adaptation capacity and also serves as a regularizer (Biderman et al., 2024). Using differential ranks therefore provides a systematic way to harmonize multimodal fine-tuning. However, identifying an optimal rank pair is challenging due to an inherent *two-fold disparity*: (1) a disparity in learning capacity, stemming from their differing parameter scales, and (2) a disparity in the required learning

budget, as each module originates from a distinct pre-trained unimodal model with its own domain gap to the downstream task. Therefore, the core challenge lies in quantifying these disparities to align the convergence dynamics of all modules.

To address this, we introduce **MARS (Multimodal Adaptive Rank Search)**, an effective and efficient procedure for identifying optimal rank pairs that ensure aligned training dynamics. The search problem is inherently difficult: the combinatorial space of rank pairs is vast, and each candidate requires full fine-tuning runs to evaluate performance, rendering naive search inefficient and impractical. To make MARS feasible prior to full fine-tuning, we draw inspiration from research on scaling laws, which have proven effective in predicting the capabilities and performance of large deep learning models (Kaplan et al., 2020; Zhang et al., 2024a; Shukor et al., 2025). These predictive models motivate a systematic data-driven approach over heuristic trial-and-error tuning. We propose dual scaling laws tailored for MLLM fine-tuning: Scaling Law-P (Performance), which predicts final task accuracy and serves as the objective function, and Scaling Law-C (Convergence), which estimates the training iterations required for each module to converge. MARS leverages these laws to prune the search space to candidates with aligned convergence and then selects the optimal rank pair based on predicted performance, thereby substantially reducing search costs while improving results.

Our main contributions are:

- We identify and provide evidence that the imbalanced training dynamics in MLLM fine-tuning, originating from a two-fold disparity, represent a key source of sub-optimal performance. To overcome this, we propose MARS, an automated algorithm that systematically mitigates the imbalance by discovering optimal, modality-specific LoRA rank pairs.
- We are the first to propose and validate dual scaling laws for MLLM fine-tuning that model performance (Scaling Law-P) and module-specific convergence time (Scaling Law-C), making the rank search feasible.
- MARS outperforms baselines with up to 12.0% higher ScienceQA accuracy and 13.2% lower LLaVA Bench perplexity, while demonstrating robust generality and an 11.5 \times reduction in total search and fine-tuning time.

2. Related Work

Fine-Tuning Strategies for MLLMs. A prominent trend in recent MLLM research is the move towards comprehensive fine-tuning of all major components—including the vision encoder, projector, and LLM backbone—to achieve state-of-the-art performance (Zhang et al., 2024b; Zhai et al., 2024; Zanella & Ben Ayed, 2024; Chen et al., 2025). This paradigm shift away from methods that keep large parts of

the model frozen stems from the growing recognition that simply connecting a vision encoder to a static, pre-trained LLM has limitations. Deeper integration, where both modalities can adapt during fine-tuning, is required to unlock more advanced reasoning capabilities (Kim et al., 2024). Given the immense scale of these models, this comprehensive adaptation is almost exclusively enabled by parameter-efficient fine-tuning methods, particularly Low-Rank Adaptation (LoRA) (Hu et al., 2022). In general, prior work adopts a uniform rank across all modules with differential learning rates, and selects the checkpoint that yields the highest accuracy (Liu et al., 2023; Li et al., 2024; Wang et al., 2024; Bai et al., 2025).

Scaling Laws. Research on scaling laws, initiated by work on LLM pre-training (Kaplan et al., 2020; Hoffmann et al., 2022b), has established that model performance scales predictably with factors like model size and data. More recent work has extended this analysis to LLM fine-tuning (Zhang et al., 2024a) and the pre-training of native multimodal models (Shukor et al., 2025; He et al., 2025), primarily focusing on predicting final task performance. However, the study of scaling laws in MLLM fine-tuning remains largely unexplored.

3. MARS Methodology

Motivation. The fine-tuning of MLLMs is often hampered by the imbalanced training dynamics between its constituent modules, leading to suboptimal performance. To clearly isolate and demonstrate this phenomenon, as illustrated in Figure 1, we designed a controlled experimental setting. While in practice these dynamics are caused by an inherent *two-fold disparity*, we sought to show the direct impact of the imbalance itself. To achieve this, we assembled a LLaVA-OneVision-0.5B* model from pre-trained unimodal components that have similar parameter counts and no prior exposure to the multimodal task. In this controlled environment, where both modules must learn the task knowledge, we intentionally induced an imbalance using differential learning rates. Setting a much lower learning rate for the VE ($lr_{ve} \ll lr_{llm}$) resulted in a clear performance bottleneck, whereas a much lower learning rate for the LLM ($lr_{llm} \ll lr_{ve}$) caused significant training instability.

The standard heuristic to mitigate this is to manually tune differential learning rates; however, this process is laborious, relying on extensive trial-and-error rather than a predictive model. While one could attempt to automate this learning rate search, we argue that a more fundamental approach lies in leveraging a more direct control available during parameter-efficient fine-tuning: *the LoRA rank*. Unlike the learning rate, which simply scales gradient updates, the LoRA rank determines the intrinsic capacity of the adaptation and acts as a powerful regularizer (Biderman

Algorithm 1 Comparison of Naive Search and MARS

```

Input :Candidate ranks  $R_{\text{options}}$ , target dataset  $D_f$ 
Output :Optimal config  $(r_{\text{ve}}^*, r_{\text{llm}}^*)$ 
 $BestPerformance \leftarrow -\infty$ 
 $CandidatePairs \leftarrow \emptyset$ 
for  $r_{\text{llm}} \in R_{\text{options}}$  do
    # --- Naive Search: Iterate over all rank pair combinations;
    # Full fine-tune to obtain accuracy. ---
    for  $r_{\text{ve}} \in R_{\text{options}}$  do
         $Perf \leftarrow FULLFINE Tuning(r_{\text{ve}}, r_{\text{llm}}, D_f)$ 
        if  $Perf > BestPerformance$  then
             $BestPerformance \leftarrow Perf$ 
             $(r_{\text{ve}}^*, r_{\text{llm}}^*) \leftarrow (r_{\text{ve}}, r_{\text{llm}})$ 
    # +++ MARS: No inner loop; Prune search space & Select
    # best VE rank  $(r_{\text{ve}}')$  for  $r_{\text{llm}}$ . +++
     $r_{\text{ve}}' \leftarrow FINDBALANCEDRANK(r_{\text{llm}})$  // SL-C
    Add  $(r_{\text{ve}}', r_{\text{llm}})$  to  $CandidatePairs$ 
     $(r_{\text{ve}}^*, r_{\text{llm}}^*) \leftarrow SELECTBEST(CandidatePairs)$  // SL-P
return  $(r_{\text{ve}}^*, r_{\text{llm}}^*)$ 

```

et al., 2024). We posit that finding an optimal pair of differential LoRA ranks is therefore a more effective approach to harmonizing multimodal fine-tuning. However, a naive (exhaustive) search for this optimal rank pair is computationally prohibitive, as each combination would require a full fine-tuning run. In this section, we introduce MARS, which addresses this challenge. We first provide an overview of our methodology, highlighting the dual scaling laws, before elaborating on the detailed search procedure.

3.1. Multimodal Adaptive Rank Search

The MARS framework is designed to transform the intractable search for optimal LoRA ranks into an efficient, guided procedure. It functions as a pre-fine-tuning stage prior to final task-specific training. As in Algorithm 1, a naive search would require a costly inner loop, executing a full fine-tuning run for every possible rank combination. MARS fundamentally improves this process by replacing this expensive inner loop with an efficient, predictive model.

The core of the search is a guided, two-step process that efficiently identifies the optimal rank pair:

- Pruning via Convergence Balancing:** First, MARS uses our convergence law (*Scaling Law-C*) to enforce a balance condition ($t_{\text{ve}} \approx t_{\text{llm}}$). This allows it to drastically prune the search space to candidate pairs predicted to exhibit stable, harmonized training dynamics.
- Selection via Performance Prediction:** Subsequently, from this pruned set of stable candidates, MARS uses our performance law (*Scaling Law-P*) to predict the final task accuracy for each pair and selects the one with the best predicted outcome.

Once fine-tuning begins, MARS first runs a lightweight calibration to fit the dual scaling law coefficients. It then enters the search phase, using predictive modeling instead of exhaustive search. This two-phase design efficiently identifies a high-performing, convergence-aware rank pair before full fine-tuning.

3.2. Dual Scaling Laws

Dual scaling laws are the predictive foundation that makes rank search feasible. In this section, we elaborate on the details of the dual scaling laws, including how they are formulated and validated in the MLLM fine-tuning setup.

3.2.1. EXPERIMENTAL SETUP

To empirically derive our scaling laws, we designed a controlled experimental setup to isolate and measure pure fine-tuning capability. Our experiments are based on the LLaVA-OneVision (OV) architecture (Li et al., 2024), but we initialize our models “from scratch.” This means we assemble publicly available vision encoder (VE) (SigLIP; Zhai et al. (2023)) and LLM (Qwen2; Wang et al. (2024)) checkpoints with a pre-trained projector, ensuring the model architecture is consistent while the initial parameters have no prior exposure to the downstream fine-tuning datasets. This controlled initialization allows us to focus solely on the scaling dynamics of the fine-tuning process itself. To study the impact of parameter disparity, we used two variants: LLaVA-OV-0.5B* (minimal VE-LLM parameter size gap) and LLaVA-OV-7B* (significant gap).

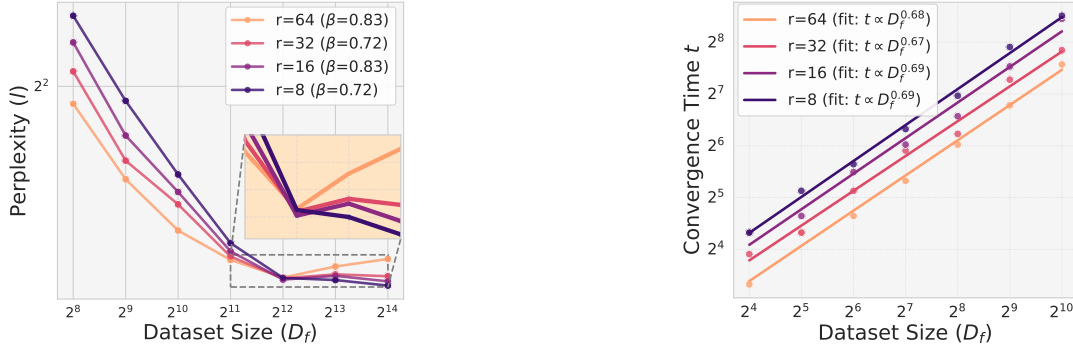
Our primary fine-tuning dataset was LLaVA-158K (Liu et al., 2023; Li et al., 2024), from which we sampled varying subset sizes to study scaling trends. We use validation perplexity as our primary metric to measure fundamental fine-tuning capability (transferability), as it directly aligns with the training objective. Experimental setup details are in Appendix A. Convergence is defined by a standard early stopping criterion (Prechelt, 2002; PyTorchIgnite): the model is considered converged if validation performance fails to improve for a set number of steps (five in this paper).

3.2.2. SCALING LAW-P FOR PERFORMANCE

Formulation. Based on our empirical findings and previous scaling laws on LLM fine-tuning (Zhang et al., 2024a), we formulate Scaling Law-P to model the fine-tuning loss (or perplexity, \hat{L}) for an MLLM. This law extends existing frameworks by incorporating separate LoRA ranks for the VE (r_{ve}) and the LLM (r_{llm}), alongside the dataset size (D_f):

$$\hat{L}(r_{\text{ve}}, r_{\text{llm}}, D_f) = A \cdot \frac{1}{(r_{\text{ve}})^{\alpha_m} \cdot (r_{\text{llm}})^{\alpha_l} \cdot D_f^\beta} + E \quad (1)$$

Here, α_m and α_l are scaling exponents for the VE and LLM ranks, reflecting their impact on loss reduction; β is the



(a) Scaling Law-P: Performance (perplexity) as a function of dataset size for different LLM ranks ($r_{ve} = 4$). The yellow line ($r_{llm} = 64$) shows that larger discrepancies between VE and LLM lead to reduced fine-tuning capability.

(b) Scaling Law-C: Convergence time as a function of dataset size for different LLM ranks ($r_{ve} = 16$). The near-parallelism of the fitted lines supports the separability of the rank and dataset size terms in Equation 2.

Figure 2. The proposed dual scaling laws from LLaVA-OV-0.5B* (VE and LLM have a similar parameter count without task-specific knowledge). This pattern holds consistently across different fixed-rank settings (e.g., $r_{ve} = 8$ and $r_{ve} = 32$).

exponent for dataset size. A and E are fitted constants representing a scaling coefficient and an irreducible error, respectively. This law serves as the objective function in MARS.

Key Observation. Scaling Law-P is grounded in the foundational scaling laws (Zhang et al., 2024a), which were originally established in the context of unimodal (LLM) fine-tuning. While this law holds under its original conditions, our work identifies a critical counterexample: *the law breaks down when there is a non-negligible imbalance in training dynamics across heterogeneous components.*

1) Performance is sensitive to the interplay between VE and LLM ranks. Unlike unimodal studies, where LoRA rank often has a modest effect, MLLM fine-tuning performance strongly depends on the combination of ranks chosen for the VE and the LLM. An imbalance between these ranks can undermine training benefits, particularly on large datasets (Figure 2a), highlighting the need to consider both ranks jointly for effective fine-tuning.

2) Optimal LoRA rank pair involves a trade-off with dataset size. Performance is non-monotonic: small datasets benefit from higher VE ranks for richer feature extraction (see Appendix D), while large datasets favor moderate ranks to avoid overfitting. Thus, the optimal rank pair balances expressive feature learning with overfitting risk, depending on dataset size.

These findings highlight the need for an adaptive, modality-aware rank search. Additional results, including counterex-

amples and justifications (e.g., why a multiplicative rather than additive formulation), are provided in Appendix E.

3.2.3. SCALING LAW-C FOR CONVERGENCE TIME

Formulation. Modeling the relationship between LoRA rank, dataset size, and convergence time (i.e., the number of iterations required for convergence) is a relatively under-explored area. To address this, we propose Scaling Law-C to model the convergence time for each modality-specific module within an MLLM. For a given module i , where i represents either the VE or the LLM, we define the convergence time t_i using the following general form:

$$t_i(r_i, D_f) = k_i \cdot (r_i)^{\gamma_i} \cdot D_f^{\delta_i} + E_i \quad (2)$$

Here, t_i is the predicted number of training steps to convergence for module i (e.g., $i \in \{ve, llm\}$), with LoRA rank r_i and dataset size D_f . The exponent $\gamma_i < 0$ captures the effect of rank on convergence time, while δ_i reflects the impact of dataset size. Constants k_i and E_i are fitted from data. This model predicts how convergence scales with rank and data, enabling MARS to balance t_{ve} and t_{llm} during pruning.

Key Observation. Our empirical results strongly support Scaling Law-C, showing consistent convergence time trends across varying dataset sizes and LoRA ranks.

1) Increasing dataset size increases convergence time. Larger fine-tuning datasets (D_f) require more iterations for the model to converge. This is intuitive, as the model needs additional steps to process and learn from the extra data. The near-linear trend, shown in Figure 2b, aligns with the $D_f^{\delta_i}$ term in Equation 2.

2) Increasing rank size *decreases* convergence time.

Modules with higher LoRA ranks (r_i) converge in fewer iterations, as larger ranks provide greater capacity and flexibility for efficient adaptation. Consequently, these modules reach convergence faster than those with lower, constrained ranks. This inverse relationship aligns with the $r_i^{\gamma_i}$ term in Equation 2, with negative γ_i capturing the acceleration.

These two distinct scaling behaviors form the empirical basis for our convergence time predictions, which are integral to MARS’s ability to identify convergence-balanced rank pairs. Additional *theoretical* and *empirical* evidence is provided in Appendix F.

3.3. The Guided Search Space Optimization

Once the dual scaling laws are calibrated, MARS performs an automated search for the optimal LoRA rank pair (r_{ve}^* , r_{llm}^*) for a target dataset size. The search first prunes the vast space of possible rank combinations using our fitted Scaling Law-C. This strategy is computationally grounded in the *monotonic smoothness* and *local continuity* of the scaling landscape observed in our evidence (see Figure 2b & Appendix F). Because the training dynamics are smooth and order-preserving without abrupt spikes or discontinuities across the search space, MARS models Scaling Law-C as a continuous power-law function, enabling efficient pruning via interpolation between discrete anchor points.

The guiding principle is to identify rank pairs where the VE and LLM modules achieve aligned convergence times ($t_{ve} \approx t_{llm}$). By leveraging the overall smoothness of these scaling curves, we can solve this balance condition to express the ideal VE rank as a direct function of the LLM rank:

$$r_{ve} \approx \left(\frac{k_l \cdot (r_{llm})^{\gamma_l} \cdot D_f^{\delta_l} + E_{llm} - E_{ve}}{k_v \cdot D_f^{\delta_v}} \right)^{\frac{1}{\gamma_v}} \quad (3)$$

To generate a set of *convergence-aligned* candidates, MARS iterates through a list of possible LLM ranks, uses Equation 3 to calculate the corresponding ideal VE rank for each, and rounds to the closest integer based on the local continuity and smoothness of the scaling landscape. This procedure efficiently creates a pruned set of candidate pairs, *CandidatePairs*, in Algorithm 1. See Appendix G for the full derivation.

The final step is to select the pair with the highest performance potential. We use the fitted Scaling Law-P to predict the fine-tuning perplexity, \hat{L} , for each candidate pair, with Θ_{acc} denoting the fitted coefficients. The optimal rank pair is the one that minimizes this predicted perplexity:

$$(r_{ve}^*, r_{llm}^*) = \underset{(r_{ve}, r_{llm}) \in \text{CandidatePairs}}{\operatorname{argmin}} \hat{L}(r_{ve}, r_{llm}, D_f; \Theta_{acc}) \quad (4)$$

The value of our dual scaling law framework lies in its synergistic two-phase approach. A search guided only by a performance predictor can yield *practically unstable* configurations due to the gradient interference caused by imbalanced convergence, while optimizing only for balance does not guarantee the highest accuracy. MARS resolves this trade-off by first using Scaling Law-C to prune the search space to a stable subset of candidates, and then employing Scaling Law-P to select the highest-performing solution from that set.

3.4. Calibration of Dual Scaling Laws

When fine-tuning begins, the MARS procedure starts with a calibration phase that empirically estimates the coefficients of our dual scaling laws. To minimize computational cost, we employ an efficient data collection strategy: for each representative LoRA rank pair (e.g., $r_{ve}, r_{llm} \in \{8, 16, 32, 64\}$), we initiate a single fine-tuning run and record performance and convergence metrics at multiple intermediate checkpoints corresponding to smaller effective dataset sizes (e.g., at 2^{10} and 2^{11} fine-tuning steps). This approach yields a rich dataset, \mathcal{D} , from a minimal number of training runs. Using this dataset, we determine the coefficients for both Scaling Law-P and Scaling Law-C by framing it as a numerical optimization problem. Following established practices (Hoffmann et al., 2022a; Zhang et al., 2024a), we employ the L-BFGS-B algorithm to find the parameter set that minimizes the Huber loss between our model’s predictions and the observed data. Crucially, this calibration stage utilizes the same fine-tuning settings (e.g., optimizer, batch size) as the full fine-tuning, ensuring the identified rank pair remains effective. The result is a reliable predictive model of performance and convergence dynamics, essential for the subsequent guided search.

4. Evaluation

4.1. Evaluation Setup

Evaluation Focus. To ensure a comprehensive assessment, we consider the overall phases of VLM fine-tuning in alignment with current community trends and established practices, which can be categorized into two types:

- **Generalist Fine-tuning.** Fine-tuning the model on a diverse set of general multimodal instructions to build a strong foundational generalist. This stage is often referred to as *pre-training* after the pre-trained VE and LLM are first connected, as these components have not previously been exposed to multimodal tasks.

Table 1. Comparison with fixed-rank tuning across different learning rates. We determined the best VE learning rate (★) for each LLM learning rate (r_{llm}) by selecting the value that yielded either the lowest perplexity or the highest accuracy. For the LLaVA Bench, lower perplexity is better (↓), while for ScienceQA, higher accuracy is better (↑). Best in bold, second-best underlined.

Model	Benchmark	LoRA (r_{ve} , r_{llm})			MARS
		(★, 1e-5)	(★, 1e-6)	(★, 1e-7)	
LLaVA-OV-0.5B (Li et al., 2024)	LLaVA (↓)	<u>2.7336</u>	2.771	2.8472	2.7188
	ScienceQA (↑)	<u>71.06</u>	61.88	59.28	72.85
LLaVA-OV-7B (Li et al., 2024)	LLaVA (↓)	2.2317	<u>2.295</u>	2.4346	2.1875
	ScienceQA (↑)	<u>72.26</u>	69.86	67.27	74.25
Qwen2.5-VL-3B (Bai et al., 2025)	LLaVA (↓)	<u>3.6156</u>	3.7415	4.1557	3.5925
	ScienceQA (↑)	<u>78.04</u>	76.45	76.25	79.24
Qwen2.5-VL-7B (Bai et al., 2025)	LLaVA (↓)	<u>3.5032</u>	3.5908	3.8716	3.3879
	ScienceQA (↑)	79.84	76.25	74.25	<u>79.64</u>

- **Specialist Fine-tuning.** Fine-tuning a pre-trained generalist model on domain-specific datasets to produce a specialized expert. This stage is generally referred to as *post-training*. Given that the model possesses strong general knowledge, effective fine-tuning must balance acquiring task-specific knowledge while preserving pre-trained representations.

Evaluation Benchmarks and Datasets. To evaluate the effectiveness of MARS, we utilize two distinct benchmarks designed to measure different types of fine-tuning performance. For generalist fine-tuning, we use LLaVA Bench (Liu et al., 2023), which consists of 15k validation samples from the LLaVA-Instruct dataset and is composed of complex reasoning tasks. For this benchmark, we use validation perplexity as the primary metric. Perplexity, computed directly from cross-entropy loss, serves as a proxy for the model’s training objective (minimizing loss) and provides a direct measure of its fine-tuning capability by indicating how well it can specialize on a downstream dataset. For specialist fine-tuning, we use the ScienceQA benchmark (Lu et al., 2022). This benchmark contains multimodal multiple-choice questions across diverse scientific subjects, including natural science, language science, and social science. For our experiments, we use a 16k training split and evaluate on 500 test samples. Following the standard evaluation protocol, we report performance using accuracy.

After an in-depth evaluation on these two benchmarks, we further extend the assessment of MARS to a broader set of benchmarks to evaluate its generality: MME (Fu et al., 2023), MMStar (Chen et al., 2024), POPE (Li et al., 2023), TextCaps (Sidorov et al., 2020), AI2D (Kembhavi et al., 2016), GQA (Hudson & Manning, 2019). Benchmark details are provided in Appendix H.

Baselines. To demonstrate the effectiveness of MARS as an adaptive rank search algorithm for convergence coordi-

Table 2. Comparison with adaptive rank search baselines. We determined the best VE rank size (★) for each LLM rank size (r_{llm}) by selecting the value that yielded either the lowest perplexity or the highest accuracy. For the LLaVA Bench, lower perplexity is better (↓), while for ScienceQA, higher accuracy is better (↑). Best in bold, second-best underlined.

Model	AdaLoRA	GeoLoRA	Full-rank Tuning	LoRA (r_{ve} , r_{llm})			MARS
				(★, 8)	(★, 16)	(★, 32)	
<i>LLaVA Bench (perplexity ↓)</i>							
LLaVA-OV-0.5B	2.8973	2.8801	<u>2.7209</u>	2.7582	2.7336	2.7331	2.7188
LLaVA-OV-7B	2.5189	2.4888	2.2693	2.3181	<u>2.2317</u>	2.4420	2.1875
Qwen2.5-VL-3B	3.6679	3.6676	3.6528	<u>3.5912</u>	3.6156	3.7811	3.5825
Qwen2.5-VL-7B	3.6394	3.6378	3.5917	<u>3.5011</u>	3.5032	3.6098	3.3616
<i>ScienceQA bench (accuracy (%) ↑)</i>							
LLaVA-OV-0.5B	62.28	63.52	69.66	70.46	<u>71.06</u>	69.86	72.85
LLaVA-OV-7B	66.27	67.81	70.46	70.26	72.26	<u>73.65</u>	74.25
Qwen2.5-VL-3B	70.06	70.46	75.25	<u>78.24</u>	78.04	78.04	79.24
Qwen2.5-VL-7B	73.85	72.85	77.45	79.84	79.84	78.24	<u>79.64</u>

nation, we compare it against several key baselines. The first is a differential learning rate approach, representing the standard heuristic of manually tuning separate learning rates for the VE and LLM. Second, since we argue that using differential ranks between modalities is important, we compare against a set of fixed differential rank pairs (i.e., uniform but different across modalities). Finally, we benchmark against AdaLoRA (Zhang et al., 2023) and GeoLoRA (Schotthöfer et al., 2024), two representative adaptive rank allocation methods designed for unimodal models. For both, we use the officially released source code (see Appendix B for details). By comparing against these methods, we demonstrate that MARS effectively identifies the optimal rank combination, resulting in improved fine-tuning performance.

Implementation Details. Our experiments are implemented using the Cornstarch MLLM training framework (Jang et al., 2025). All models were fine-tuned using the Adam optimizer with a cosine learning rate scheduler, and all experiments were conducted on a single NVIDIA GH200 GPU. Further details regarding specific hyperparameters, LoRA configurations, and the MARS calibration setup are provided in Appendix C.

4.2. Main Results

We evaluate MARS across multiple MLLM architectures and model scales, comparing it against several strong baselines across various benchmarks. As shown in Tables 1 and 2 and Figure 3, the fine-tuned models with MARS show effectiveness and generality compared to our baselines.

Comparison with Differential Learning Rates. Table 1 compares MARS against the common heuristic of using fixed LoRA ranks while tuning differential learning rates. On the LLaVA Bench, MARS consistently achieves a lower (better) perplexity across all tested models. For instance, on the LLaVA-OV-7B model, MARS achieves a perplexity of

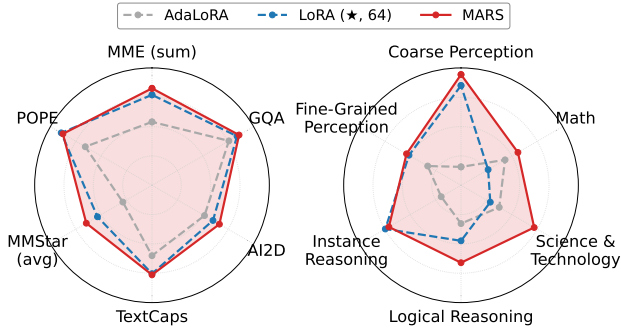


Figure 3. Evaluation of Generalist Capabilities. **Left:** Comparison across diverse multimodal benchmarks demonstrating broad generalization. **Right:** Fine-grained capability breakdown on MMStar. Detailed numbers are in Appendix H.2.

2.1875, outperforming the best-performing differential LR setting (2.295). This trend holds on the more specialized ScienceQA benchmark, where MARS improves the accuracy of the LLaVA-OV-7B model from 72.26% to 74.25%. These results demonstrate that our rank-centric search is a more effective strategy for harmonizing module dynamics than just tuning learning rates.

Comparison with Other Baselines. In Table 2, we benchmark MARS against a wider range of fine-tuning strategies. MARS consistently surpasses Full-rank Tuning, highlighting the regularization benefits of our adaptive PEFT approach. More importantly, it outperforms various fixed differential LoRA rank pairs, proving the value of our guided search over simply selecting arbitrary rank combinations. The most critical comparison is with AdaLoRA and GeoLoRA, both representative adaptive-rank methods designed for unimodal models. MARS significantly and consistently outperforms these methods across all models and benchmarks. This confirms that methods designed for single-modality, layer-wise saliency are insufficient for the unique challenge of harmonizing the training dynamics between different modalities in MLLMs.

Generality of MARS with Broader Benchmark Coverage. To demonstrate the generality of MARS, we evaluate the model on a diverse set of benchmarks, including both generic and domain-specific tasks. Given the limited data diversity of the initial LLaVA dataset (Liu et al., 2023), we use the updated version, LLaVA-1.5-665K (Liu et al., 2024a), to train LLaVA-OV-7B*. This experiment is generalist fine-tuning with a from-scratch model, isolating pre-trained knowledge to assess MARS’s generality. As shown in Figure 3, MARS mostly outperforms the strongest LoRA baselines (rank combinations $r_{ve} \in \{32, 48, 64\}$, $r_{llm} = 64$) and adaptive methods such as AdaLoRA (target rank= 64) across the benchmarks. For this experiment, we set $R_{options}$ (i.e., candidate ranks for the LLM) to $\{32, 48, 64\}$ to better absorb the knowledge from the large, diverse dataset.

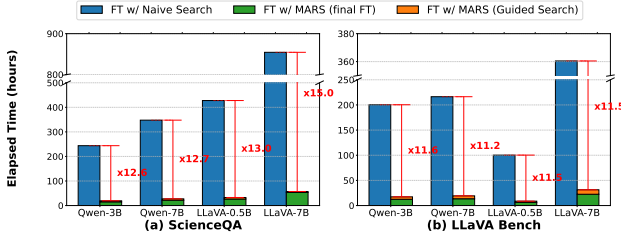


Figure 4. Time comparison between Naive Search and MARS. Naive Search explores the grid $\{4, 8, 16, 32\} \times \{4, 8, 16, 32\}$ to find the optimal rank pair (r_{ve}, r_{llm}) . MARS accounts for both the search time and the full fine-tuning time of the selected rank pair.

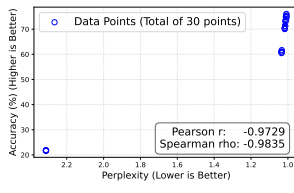


Figure 5. Correlation between Perplexity and Task Accuracy.

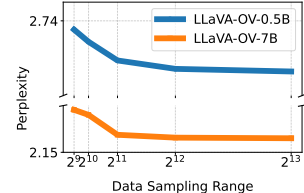


Figure 6. Impact of Data Sampling Range.

4.3. Computational Efficiency

Beyond its advantages in fine-tuning effectiveness, MARS also achieves a substantial improvement in computational efficiency. As shown in Figure 4, a naive exhaustive search for the optimal rank pair requires extensive compute, often exceeding 100 GPU hours. In contrast, MARS consists of a lightweight calibration phase followed by a single fine-tuning run, reducing the total elapsed time by more than 11.5x on average across different models and tasks, with most of the time spent on the actual fine-tuning (which is unavoidable). This substantial reduction in search cost demonstrates that MARS is not only more effective, but also more practical and scalable for MLLM fine-tuning.

4.4. Impact of Convergence Alignment on Performance

To validate the hypothesis that aligning the convergence times of the Vision Encoder (VE) and the Large Language Model (LLM) leads to better final performance, we performed a two-part statistical analysis linking convergence synchronization, perplexity, and final accuracy.

Perplexity as a Performance Proxy. First, we establish the reliability of perplexity as a robust, task-agnostic proxy

Table 3. Statistical correlation between the Convergence Gap ($|T_{ve} - T_{llm}|$) and Perplexity across varying data scales.

Dataset Size	Pearson’s r	P-value
0.5K	0.90	0.0020
1K	0.95	0.0003
2K	0.87	0.0052
4K	0.98	0.0000
8K	0.96	0.0009

Table 4. Comparison with fixed-rank tuning across different learning rates using from-scratch models. Details as in Table 1.

Model	Benchmark	LoRA (r_{ve}, r_{lm})			MARS
		(★, 1e-5)	(★, 1e-6)	(★, 1e-7)	
LLaVA-OV-0.5B*	LLaVA (↓)	<u>5.0011</u>	5.0209	5.4407	4.9547
	ScienceQA (↑)	<u>42.49</u>	42.12	39.88	45.01
LLaVA-OV-7B*	LLaVA (↓)	<u>3.8701</u>	4.0298	4.3407	3.5609
	ScienceQA (↑)	63.71	<u>64.11</u>	60.24	65.07
Qwen2-VL-7B*	LLaVA (↓)	<u>3.7738</u>	3.7949	4.0315	3.6214
	ScienceQA (↑)	<u>65.47</u>	62.87	59.28	66.47

for fine-tuning quality. While prior studies (Li et al., 2024; Shukor et al., 2025) already suggest a link between lower perplexity and improved downstream performance, we empirically validate this relationship in our fine-tuning setup using the ScienceQA dataset. Figure 5 shows a strong negative correlation between test perplexity and task accuracy (Pearson’s $r = -0.97, p < .001$), confirming that optimizing the perplexity proxy effectively maximizes task accuracy.

Linking Convergence Gap to Performance. Building on this proxy, we directly addressed the relationship between the *Convergence Gap* ($|T_{ve} - T_{lm}|$) and model perplexity. We conducted a statistical correlation analysis across multiple fine-tuning regimes with dataset sizes ranging from $D = 2^9$ to 2^{13} . As in Table 3, we observed statistically significant positive correlations ($r > 0.86, p < 0.01$) across all scales. These results confirm that minimizing the convergence gap is a statistically dominant predictor of reduced perplexity and, by extension, superior model performance.

4.5. Ablation: Evaluation on From-Scratch MLLMs.

To assess pure fine-tuning capability, we evaluate task performance on from-scratch models whose modules have not been exposed to multimodal training data. Since the original from-scratch models are not publicly available (Li et al., 2024; Wang et al., 2024), we instead assemble unimodal models and connect them with a projector to replicate the reference architectures (Sec. 3.2.1). As shown in Tables 4 and 5, MARS consistently outperforms the baseline configurations, highlighting its effectiveness in enabling from-scratch models to acquire downstream knowledge.

4.6. Ablation: Impact of Data Sampling Range.

We conducted an ablation study to determine the optimal range of data required for the lightweight calibration phase of MARS. We ran the MARS search procedure multiple times, each time using a different maximum data sampling range for calibration, and then evaluated the final test perplexity achieved by the resulting optimal rank pair. As shown in Figure 6, we observe that increasing the data sampling range up to 2^{11} leads to a clear improvement in the final perplexity, as it allows for a more accurate fitting of the scaling laws. However, performance gains diminish significantly beyond that point, validating our choice of using a data sampling range up to 2^{11} for MARS calibra-

Table 5. Comparison with adaptive rank search baselines using from-scratch models. Details as in Table 2.

Model	AdaLoRA	LoRA (r_{ve}, r_{lm})			MARS
		(★, 8)	(★, 16)	(★, 32)	
<i>LLaVA Bench (perplexity ↓)</i>					
LLaVA-OV-0.5B*	5.0807	5.2819	5.0011	<u>4.9912</u>	4.9547
LLaVA-OV-7B*	4.0012	<u>3.6175</u>	3.8701	3.9204	3.5609
Qwen2-VL-7B*	4.1555	<u>3.7480</u>	3.7738	4.1057	3.6214
<i>ScienceQA bench (accuracy (%) ↑)</i>					
LLaVA-OV-0.5B*	41.52	38.27	<u>42.49</u>	41.99	45.01
LLaVA-OV-7B*	58.28	64.11	<u>64.15</u>	64.07	65.07
Qwen2-VL-7B*	60.08	<u>65.87</u>	65.47	63.67	66.47

tion, as it strikes an effective balance between accuracy and computational efficiency.

5. Discussion

Scalability with Modality Expansion. We address the combinatorial explosion of multimodal hyperparameter tuning by ensuring MARS scales linearly ($O(N)$) with the number of modalities, in contrast to the exponential growth ($O(C^N)$) of naive grid search. By anchoring the LLM rank as a reference, MARS transforms the search into $(N - 1)$ independent 1D equations. Furthermore, to minimize the overhead of the calibration phase, we employ a Simultaneous Multi-Rank Adapter Tuning strategy (see Appendix I). By leveraging a frozen backbone with multiple parallel adapters, we reduce the calibration cost to near-constant time $O(1)$, ensuring that MARS remains computationally efficient even as the number of modalities scales.

Adaptivity to Diverse Scenarios. Beyond efficiency, MARS demonstrates robust adaptivity across distinct fine-tuning regimes. Our empirical results confirm that the method dynamically allocates ranks to address specific constraints, including limited pre-training alignment, low-data regimes, and large domain shifts. This flexibility is further supported by the observed smoothness of scaling laws, which justifies our continuous rank interpolation method for precise, fine-grained adjustments.

6. Conclusion

We introduce MARS to address imbalanced convergence in MLLM fine-tuning. By leveraging dual scaling laws to predict convergence and prune the LoRA rank search space, MARS identifies optimal rank pairs with balanced dynamics and outperforms common heuristic-based strategies, highlighting the importance of convergence coordination for effective multimodal adaptation. As future work, we aim to systematically characterize the fine-grained relationships between domain sensitivity across pre-training and fine-tuning tasks, modality-specific learning capacity disparities, and their impact on training dynamics and system-level efficiency.

7. Impact Statements

As MLLMs become more integrated into real-world applications, their adoption through fine-tuning is becoming increasingly popular across a wider range of downstream domains. The optimal rank pair identified by MARS reduces fine-tuning costs by eliminating the repetitive fine-tuning process caused by laborious trial-and-error hyperparameter searches. Ultimately, MARS will accelerate the development cycle and lower the carbon footprint for large-scale MLLM fine-tuning.

References

- Allen-Zhu, Z. and Li, Y. Physics of language models: Part 3.3, knowledge capacity scaling laws, 2024. URL <https://arxiv.org/abs/2404.05405>, pp. 2, 2023.
- Bai, S., Chen, K., Liu, X., Wang, J., Ge, W., Song, S., Dang, K., Wang, P., Wang, S., Tang, J., et al. Qwen2. 5-vl technical report. *arXiv preprint arXiv:2502.13923*, 2025.
- Biderman, D., Portes, J., Ortiz, J. J. G., Paul, M., Greengard, P., Jennings, C., King, D., Havens, S., Chiley, V., Frankle, J., et al. Lora learns less and forgets less. *arXiv preprint arXiv:2405.09673*, 2024.
- Chen, L., Li, J., Dong, X., Zhang, P., Zang, Y., Chen, Z., Duan, H., Wang, J., Qiao, Y., Lin, D., et al. Are we on the right way for evaluating large vision-language models? *arXiv preprint arXiv:2403.20330*, 2024.
- Chen, X., Wu, Z., Liu, X., Pan, Z., Liu, W., Xie, Z., Yu, X., and Ruan, C. Janus-pro: Unified multimodal understanding and generation with data and model scaling. *arXiv preprint arXiv:2501.17811*, 2025.
- Dong, Z., Yao, Z., Gholami, A., Mahoney, M. W., and Keutzer, K. Hawq: Hessian aware quantization of neural networks with mixed-precision. In *Proceedings of the IEEE/CVF international conference on computer vision*, pp. 293–302, 2019.
- Ed-dib, A., Datbayev, Z., and Aboussalah, A. M. Gelora: Geometric adaptive ranks for efficient lora fine-tuning. *arXiv preprint arXiv:2412.09250*, 2024.
- Fu, C., Chen, P., Shen, Y., Qin, Y., Zhang, M., Lin, X., Yang, J., Zheng, X., Li, K., Sun, X., et al. Mme: A comprehensive evaluation benchmark for multimodal large language models. *arXiv preprint arXiv:2306.13394*, 2023.
- He, S., Jang, I., and Chowdhury, M. Mordal: Automated pre-trained model selection for vision language models, 2025. URL <https://arxiv.org/abs/2502.00241>.
- Hoffmann, J., Borgeaud, S., Mensch, A., Buchatskaya, E., Cai, T., Rutherford, E., Casas, D. d. L., Hendricks, L. A., Welbl, J., Clark, A., et al. Training compute-optimal large language models. *arXiv preprint arXiv:2203.15556*, 2022a.
- Hoffmann, J., Borgeaud, S., Mensch, A., Buchatskaya, E., Cai, T., Rutherford, E., Casas, D. d. L., Hendricks, L. A., Welbl, J., Clark, A., et al. Training compute-optimal large language models. *arXiv preprint arXiv:2203.15556*, 2022b.
- Hu, E. J., Shen, Y., Wallis, P., Allen-Zhu, Z., Li, Y., Wang, S., Wang, L., Chen, W., et al. Lora: Low-rank adaptation of large language models. *ICLR*, 1(2):3, 2022.
- Hudson, D. A. and Manning, C. D. Gqa: A new dataset for real-world visual reasoning and compositional question answering. *Conference on Computer Vision and Pattern Recognition (CVPR)*, 2019.
- Jang, I., Lu, R., Bansal, N., Chen, A., and Chowdhury, M. Cornstarch: Distributed multimodal training must be multimodality-aware. *arXiv preprint arXiv:2503.11367*, 2025.
- Kaplan, J., McCandlish, S., Henighan, T., Brown, T. B., Chess, B., Child, R., Gray, S., Radford, A., Wu, J., and Amodei, D. Scaling laws for neural language models. *arXiv preprint arXiv:2001.08361*, 2020.
- Ke, W., Wang, J., Wang, P., Liu, J., Nie, D., Li, G., and Li, Y. Unveiling lora intrinsic ranks via salience analysis. *Advances in Neural Information Processing Systems*, 37: 131575–131595, 2024.
- Kembhavi, A., Salvato, M., Kolve, E., Seo, M., Hajishirzi, H., and Farhadi, A. A diagram is worth a dozen images. In *European conference on computer vision*, pp. 235–251. Springer, 2016.
- Kim, M. J., Pertsch, K., Karamcheti, S., Xiao, T., Balakrishna, A., Nair, S., Rafailov, R., Foster, E., Lam, G., Sanke, P., et al. Openvla: An open-source vision-language-action model. *arXiv preprint arXiv:2406.09246*, 2024.
- Lee, D., Cho, M., Lee, S., Song, J., and Choi, C. A novel sensitivity metric for mixed-precision quantization with synthetic data generation. In *2021 IEEE International Conference on Image Processing (ICIP)*, pp. 1294–1298. IEEE, 2021.
- Li, B., Zhang, Y., Guo, D., Zhang, R., Li, F., Zhang, H., Zhang, K., Zhang, P., Li, Y., Liu, Z., et al. Llava-onevision: Easy visual task transfer. *arXiv preprint arXiv:2408.03326*, 2024.
- Li, Y., Du, Y., Zhou, K., Wang, J., Zhao, W. X., and Wen, J.-R. Evaluating object hallucination in large vision-language models. *arXiv preprint arXiv:2305.10355*, 2023.

- Liu, H., Li, C., Wu, Q., and Lee, Y. J. Visual instruction tuning. *Advances in neural information processing systems*, 36:34892–34916, 2023.
- Liu, H., Li, C., Li, Y., and Lee, Y. J. Improved baselines with visual instruction tuning. In *Proceedings of the IEEE/CVF conference on computer vision and pattern recognition*, pp. 26296–26306, 2024a.
- Liu, S.-Y., Wang, C.-Y., Yin, H., Molchanov, P., Wang, Y.-C. F., Cheng, K.-T., and Chen, M.-H. Dora: Weight-decomposed low-rank adaptation. In *Forty-first International Conference on Machine Learning*, 2024b.
- Lu, P., Mishra, S., Xia, T., Qiu, L., Chang, K.-W., Zhu, S.-C., Tafjord, O., Clark, P., and Kalyan, A. Learn to explain: Multimodal reasoning via thought chains for science question answering. In *The 36th Conference on Neural Information Processing Systems (NeurIPS)*, 2022.
- Mu, S. and Klabjan, D. On the convergence rate of lora gradient descent. *arXiv preprint arXiv:2512.18248*, 2025.
- Prechelt, L. Early stopping-but when? In *Neural Networks: Tricks of the trade*, pp. 55–69. Springer, 2002.
- PyTorchIgnite. Pytorch ignite: Earlystopping.
- Schotthöfer, S., Zangrando, E., Ceruti, G., Tudisco, F., and Kusch, J. Geolora: Geometric integration for parameter efficient fine-tuning. *arXiv preprint arXiv:2410.18720*, 2024.
- Shukor, M., Fini, E., da Costa, V. G. T., Cord, M., Susskind, J., and El-Nouby, A. Scaling laws for native multimodal models. *arXiv preprint arXiv:2504.07951*, 2025.
- Shuttleworth, R., Andreas, J., Torralba, A., and Sharma, P. Lora vs full fine-tuning: An illusion of equivalence. *arXiv preprint arXiv:2410.21228*, 2024.
- Sidorov, O., Hu, R., Rohrbach, M., and Singh, A. Textcaps: a dataset for image captioning with reading comprehension. 2020.
- Team, Q. Qwen2 technical report. *arXiv preprint arXiv:2407.10671*, 2, 2024.
- Wang, P., Bai, S., Tan, S., Wang, S., Fan, Z., Bai, J., Chen, K., Liu, X., Wang, J., Ge, W., et al. Qwen2-vl: Enhancing vision-language model’s perception of the world at any resolution. *arXiv preprint arXiv:2409.12191*, 2024.
- Zanella, M. and Ben Ayed, I. Low-rank few-shot adaptation of vision-language models. In *Proceedings of the IEEE/CVF Conference on Computer Vision and Pattern Recognition Workshops*, pp. 1593–1603, 2024.
- Zhai, S., Bai, H., Lin, Z., Pan, J., Tong, P., Zhou, Y., Suhr, A., Xie, S., LeCun, Y., Ma, Y., et al. Fine-tuning large vision-language models as decision-making agents via reinforcement learning. *Advances in neural information processing systems*, 37:110935–110971, 2024.
- Zhai, X., Mustafa, B., Kolesnikov, A., and Beyer, L. Sigmoid loss for language image pre-training. In *Proceedings of the IEEE/CVF international conference on computer vision*, pp. 11975–11986, 2023.
- Zhang, B., Liu, Z., Cherry, C., and Firat, O. When scaling meets llm finetuning: The effect of data, model and finetuning method. *arXiv preprint arXiv:2402.17193*, 2024a.
- Zhang, H., Gao, M., Gan, Z., Dufter, P., Wenzel, N., Huang, F., Shah, D., Du, X., Zhang, B., Li, Y., et al. Mml. 5: Methods, analysis & insights from multimodal llm fine-tuning. *arXiv preprint arXiv:2409.20566*, 2024b.
- Zhang, K., Li, B., Zhang, P., Pu, F., Cahyono, J. A., Hu, K., Liu, S., Zhang, Y., Yang, J., Li, C., and Liu, Z. Lmms-eval: Reality check on the evaluation of large multimodal models, 2024c. URL <https://arxiv.org/abs/2407.12772>.
- Zhang, Q., Chen, M., Bukharin, A., Karampatziakis, N., He, P., Cheng, Y., Chen, W., and Zhao, T. Adalora: Adaptive budget allocation for parameter-efficient fine-tuning. *arXiv preprint arXiv:2303.10512*, 2023.

Appendix

A. Additional Experimental Details for Section 3.2

A.1. Model Setup

Our target model architecture is LLaVA-OneVision (LLaVA-OV; (Li et al., 2024)). For these scaling law experiments, all models were initialized “from scratch,” a methodology we denote with an asterisk (*). This process involves downloading publicly available, pre-trained vision encoder (VE) and Large Language Model (LLM) checkpoints and connecting them with a MLP projector, without any subsequent instruction tuning. Specifically, we used SigLIP (Zhai et al., 2023) for the VE and Qwen2 (Team, 2024) for the LLM and attached a 2-layer MLP projector to replicate the original structure.

This approach is intentionally designed to ensure that the model’s initial state is *domain-knowledge-free* with respect to multimodal instruction data. By doing so, we can isolate and measure the effects of pure fine-tuning capability as a function of data and model scale. We investigated two architectural variants to analyze the impact of the parameter gap between the VE and LLM components.

- **LLaVA-OV-0.5B***: Features a *minimal* parameter gap (VE \sim 400M, LLM \sim 500M).
- **LLaVA-OV-7B***: Features a *significant* parameter gap (VE \sim 400M, LLM \sim 7B).

A.2. Dataset Setup

Our primary dataset is the LLaVA dataset (Liu et al., 2023; Li et al., 2024), which, to our knowledge, is one of the largest of its kind available for research. Each sample is centered on images of nature or everyday life. The dataset comprises a mixture of open-ended task types, including basic image captioning, detailed image captioning, and multi-turn conversational question answering.

To study scaling trends, we constructed training subsets from this dataset by varying their size according to a power-of-two progression (i.e., 2^n samples, for n from 3 to 15), while maintaining a consistent distribution of the above task types across all subsets. For validation, we used a fixed subset of 500 samples (non-overlapping with training data) to enable frequent, low-cost perplexity checks during intermediate training cycles.

B. Additional Related Work

Adaptive LoRA for Unimodal Models. To move beyond static configurations, adaptive LoRA methods like AdaLoRA (Zhang et al., 2023), SalientLoRA (Ke et al., 2024), and GeoLoRA (Schotthöfer et al., 2024) were developed. However, these methods are designed for unimodal models and face fundamental limitations in multimodal setups. In the unimodal context, it is often observed that allocating a higher rank to more salient layers correlates with improved transferability and performance (Biderman et al., 2024), paralleling model compression techniques that allocate more resources to higher-importance components (Dong et al., 2019; Lee et al., 2021). In contrast, we found that for MLLMs, simply assigning higher ranks does not invariably lead to better performance. This is due to the complex and crucial inter-modality dependencies, where the optimal configuration for one modality is influenced by the state of the other.

C. MARS Implementation Details

C.1. General Training Hyperparameters

Unless otherwise specified, all fine-tuning experiments were conducted with the following hyperparameters. We used the Adam optimizer with its default parameter settings and a batch size of 8. The learning rate was initialized to 1×10^{-5} and followed a cosine decay schedule with a warmup phase corresponding to 10% of the total training steps. These settings were applied consistently across all experiments, with the exception of the peak learning rate in the baseline tests for differential learning rates. Following a prior paper (Liu et al., 2023), we trained for 3 epochs on the LLaVA task and 12 epochs on the ScienceQA task, reporting the best performance.

C.2. LoRA Configuration

For all experiments utilizing LoRA, we applied LoRA to all linear layers across the entire model, excluding the output heads. The LoRA scaling hyperparameter, α , was consistently set to twice the rank size (i.e., $\alpha = 2 \times r$) (Liu et al., 2024b). The initial calibration phase for MARS was performed using a representative set of LoRA ranks, $r \in \{8, 16, 32, 64\}$, for both the VE and LLM modules. We treat the projector as part of the vision encoder because it processes the same input stream for the same semantic purpose, so its adapter has the rank size of r_{ve} .

C.3. MARS Edge Case Handling

We consider rare failure cases of the MARS rank search mechanism. Specifically, in very rare cases (0.72% of all runs), the computed rank becomes complex-valued. This occurs when E_{ve} is excessively large due to the inherent entropy of the data distribution. In such cases, we fall back to a default LoRA configuration by setting $r_{ve} = r_{llm}$.

D. Optimal VE Rank Size in the Small-Dataset Regime

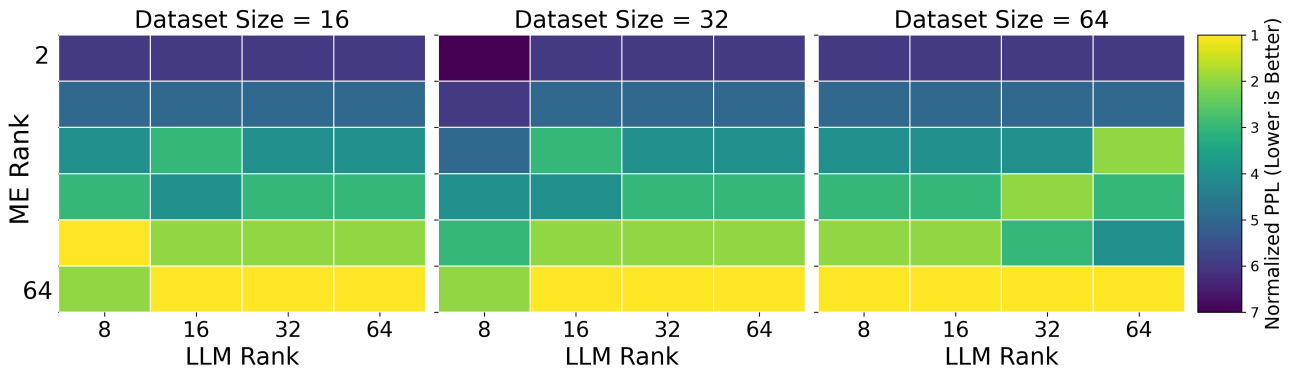


Figure 7. Optimal VE rank size in the small-dataset regime. Lower values (lighter colors) indicate better performance (i.e., lower perplexity).

The optimal VE rank is strongly dependent on the dataset size, revealing a critical trade-off between rapid adaptation and overfitting. As illustrated in the heatmaps (Figure 7), small-dataset regimes clearly prefer higher VE ranks. This is because the VE initially faces a large domain gap, and a higher rank provides the necessary adaptation capacity to quickly align with the LLM. From a capacity perspective, this aggressive approach allows the VE to absorb all available knowledge from limited samples, preventing it from becoming an early learning bottleneck.

Conversely, in mid-to-large dataset regimes, a different pattern emerges: the preference shifts to smaller or more moderate VE ranks. The primary goal becomes reducing overfitting risk and ensuring the efficient utilization of model capacity. With a large and diverse set of examples, extreme adaptation capacity is no longer required. Instead of attempting to absorb all available knowledge, a moderate rank is sufficient to extract essential visual information without over-specializing on training examples. This provides the LLM with stable, moderately adapted inputs, which promotes balanced convergence, prevents overfitting, and allows the model to fully leverage the LLM’s capacity for optimal modality harmonization.

E. Further Validation on Scaling Law-P

Formulation. We formulate Scaling Law-P to model the fine-tuning loss (or perplexity, \hat{L}) for an MLLM. This law extends existing frameworks by incorporating separate LoRA ranks for the vision encoder (r_{ve}) and the LLM (r_{llm}), alongside the dataset size (D_f):

$$\hat{L}(r_{ve}, r_{llm}, D_f) = A \cdot \frac{1}{(r_{ve})^{\alpha_m} \cdot (r_{llm})^{\alpha_l} \cdot D_f^\beta} + E \quad (5)$$

Here, α_m and α_l are scaling exponents for the VE and LLM ranks, reflecting their impact on loss reduction, while β is the

exponent for dataset size. A and E are fitted constants representing a scaling coefficient and an irreducible error, respectively.

Scaling Law-P is grounded in the foundational scaling laws proposed by prior work (Zhang et al., 2024a), which were originally established in the context of unimodal LLM fine-tuning. Consequently, their scaling formulation resembles Equation 5, but treats r_{ve} and r_{llm} collectively as a single rank parameter r . **While this law holds under its original conditions, our work identifies a critical counterexample:** the law breaks down when there is a non-negligible imbalance in training dynamics across heterogeneous components (e.g., Vision Encoder vs. LLM).

Why Multiplicative (i.e., $r_{ve} \cdot r_{llm}$)? We model the interaction as multiplicative because the VE and the LLM form a serial (not parallel) information-processing chain. A capacity bottleneck in the upstream encoder (r_{ve}) imposes an irreversible loss of information that strictly bounds the maximum performance achievable by the downstream LLM, regardless of the LLM’s capacity (Ed-dib et al., 2024). Also, following (Zhang et al., 2024a), we compare the fitting error and find that a multiplicative formulation provides a better fit than an additive one.

E.1. Empirical Evidence as a Counterexample to the Original Scaling Laws

Figure 8 provides empirical evidence for Scaling Law-P across a diverse range of experimental setups:

- **Architectures:** From balanced-capacity models (LLaVA-OV-0.5B) to highly asymmetric-capacity models (Qwen2-VL-7B and LaVA-OV-7B).
- **Task Types:** Spanning open-ended general tasks (LLaVA Bench) to close-ended domain-specific reasoning tasks (ScienceQA and OCR).

Across all settings, deviations from the standard scaling law consistently indicate the emergence of this dynamic imbalance. Specifically, we observe that when $t_{ve} \ll t_{llm}$ (or vice versa), the standard power-law prediction fails, leading to abrupt increases in perplexity in the large-data regime. This phenomenon suggests a regime of destructive interference, where the faster-converging module begins to overfit before the slower module has adequately adapted.

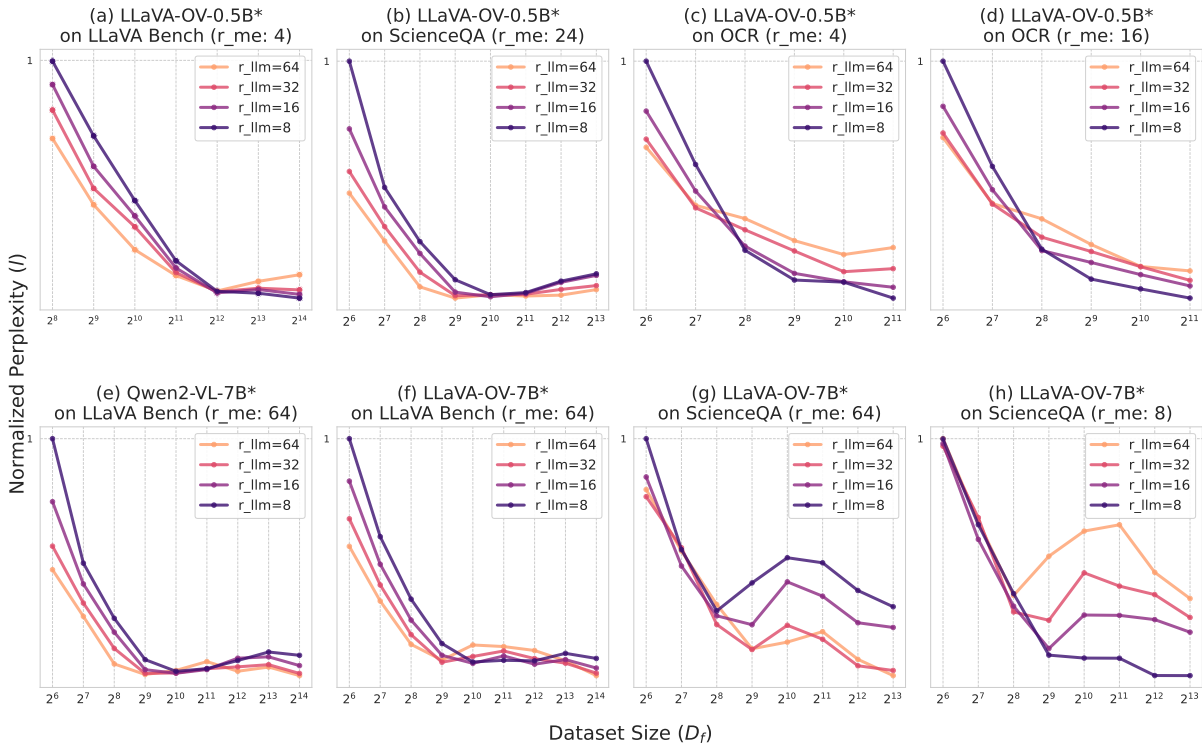


Figure 8. Validating Scaling Law-P Across Different Fine-Tuning Setups. Here, r_{me} refers to r_{ve} .

F. Further Validation on Scaling Law-C: Theoretical and Empirical Generality

We propose Scaling Law-C to estimate the computational cost of convergence, t . We model t as a tension between the **volume of information** to be absorbed (D_f) and the **condition number** of the optimization landscape (r).

Formulation. Modeling the relationship between LoRA rank, dataset size, and the number of iterations required for convergence is a relatively underexplored area. To address this, we propose Scaling Law-C to model the convergence time for each modality-specific module within an MLLM. For a given module i , where i can represent a vision encoder (VE) or the LLM, we define the number of training steps to convergence, t_i , with the following general form:

$$t_i(r_i, D_f) = k_i \cdot (r_i)^{\gamma_i} \cdot D_f^{\delta_i} + E_i \quad (6)$$

In this formulation, t_i is the predicted training steps to convergence for module i (e.g., $i \in \{\text{ve}, \text{llm}\}$). The LoRA rank for this module is r_i , and D_f is the fine-tuning dataset size. The exponent γ_i links the LoRA rank to convergence time; based on our observations that higher ranks reduce the number of steps, we fit this as a negative value. The exponent δ_i quantifies the impact of dataset size on convergence steps. Finally, k_i and E_i are constants fitted from experimental data for each module. This general formulation allows us to predict how the convergence time of any modality scales with its allocated LoRA rank and the amount of training data.

F.1. Theoretical Justification

1. **Information Absorption** ($t \propto D_f^\delta$): Convergence time scales positively with dataset size ($\delta > 0$). We ground this in *Knowledge Capacity Scaling Laws* (Allen-Zhu & Li, 2023), which establish that neural networks are bounded by a storage limit of approximately 2 bits of knowledge per parameter. As the dataset size D_f increases, the total information content grows, pushing the fixed-rank adapter toward capacity saturation. To compress this increased entropy into the limited parameter budget, the optimizer requires a longer trajectory to resolve conflicting gradients and reach a generalization minimum, leading to the observed power-law increase in steps.
2. **Geometric Conditioning** ($t \propto r^{-\gamma}$): Convergence time scales inversely with rank ($\gamma > 0$). While Mu & Klabjan (2025) suggests that the theoretical worst-case convergence rate is rank-independent under ideal assumptions, our focus is more on the premise that rank fundamentally alters the *geometry* of the loss landscape in practice.
 - *Stationary Point vs. Performance Threshold*: Previous analysis defines convergence as reaching *any* stationary point; under this definition, the convergence rate is rank-independent (Mu & Klabjan, 2025). However, Scaling Law-C models the time to reach a specific *performance threshold*. Higher ranks are necessary to bridge the *intrinsic dimension* gap, allowing the model to traverse toward the global optimum rather than stalling in rank-deficient local minima (Ed-dib et al., 2024).
 - *Spectral Stability*: Shuttleworth et al. (2024) provides spectral evidence that low-rank constraints fundamentally alter the stability of weight updates. They find that low-rank adapters exhibit lower *effective rank* (information density) compared to full fine-tuning. Increasing r increases the effective rank of the update matrix, improving *spectral stability* and ensuring smoother optimization dynamics that approximate full-rank behavior.
 - *Geometric Conditioning*: Furthermore, higher ranks mitigate the formation of *Intruder Dimensions*, which are high-magnitude singular vectors orthogonal to the pre-trained weights that appear in constrained low-rank regimes (Shuttleworth et al., 2024). Low-rank models rely on these spectral anomalies, resulting in optimization instability and forgetting. Increasing the rank expands the optimization subspace, eliminating these artifacts and improving the condition number of the landscape. This accelerates the effective velocity of convergence ($t \downarrow$) by allowing the update trajectory to align with the smoother, pre-trained spectral manifold.

Theoretically, this parallelism indicates that the geometric conditioning induced by the rank ($r^{-\gamma}$) acts as an independent multiplicative preconditioner to the information complexity of the dataset (D_f^δ). This supports our *Subspace Optimization* hypothesis by decomposing the convergence time into two orthogonal factors.

F.2. Additional Empirical Evidence

To demonstrate that this behavior reflects a fundamental property of low-rank adaptation, we investigate the Scaling Law-P pattern on the LLaVA-OneVision-0.5B and Qwen2.5-VL families (3B and 7B) using the ScienceQA dataset (Figures 9 and 10). Consistent with the results observed in Figure 2b, the Qwen2.5-VL models exhibit a near-linear relationship on the log-log scale, validating the power-law form $t \propto D^\delta$. Moreover, the fitted lines corresponding to different LoRA ranks remain nearly parallel across all architectures, providing strong empirical evidence for the separability of the rank and dataset size terms in the proposed scaling law (Equation 6).

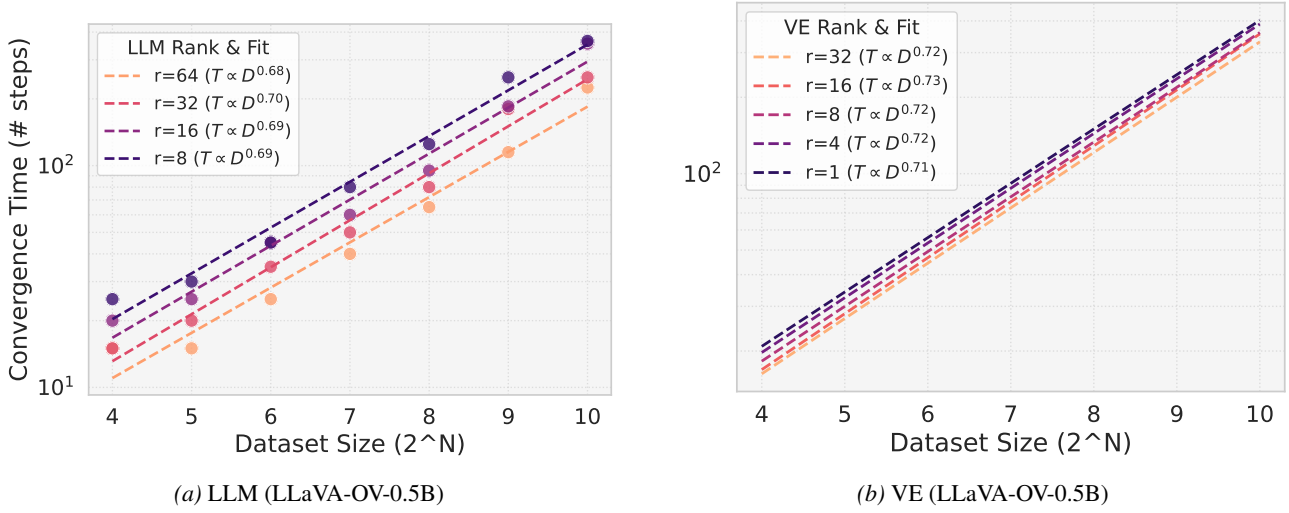


Figure 9. Scaling Law-C Validation: LLaVA-OV-0.5B Models for the ScienceQA Dataset

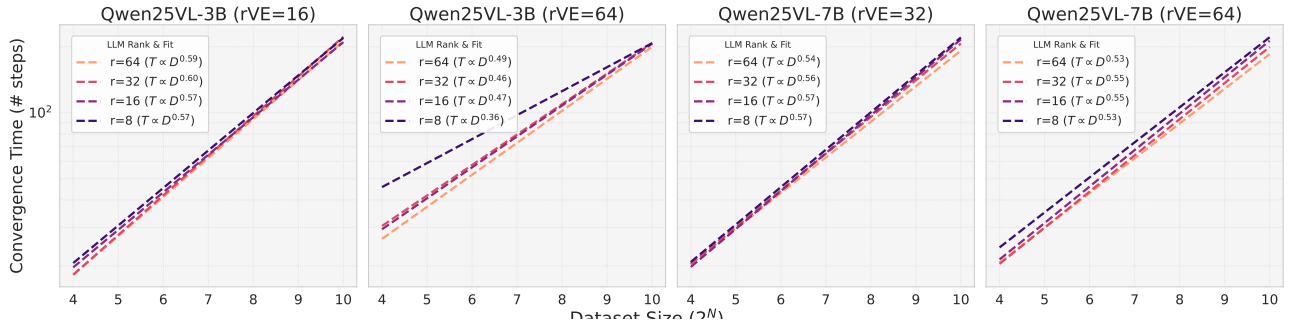


Figure 10. Scaling Law-C Validation: Qwen2.5-VL Models for the ScienceQA Dataset

G. Derivation of Equation 3

The objective of MARS is to minimize the gradient conflict caused by asynchronous convergence. By equating the convergence times derived from Scaling Law-C ($t_{ve} \approx t_{llm}$), we analytically solve for the optimal rank ratio. This ensures that both the visual perception and reasoning modules traverse their optimization manifolds at compatible velocities, preventing the fast module from overfitting while the slow module is still acquiring features.

This section provides a step-by-step derivation of Equation 3, which estimates the ideal VE-to-LLM parameter ratio (r_{ve}). The idea ratio is defined as the value that balances the expected training time of the vision encoder (t_{ve}) and the LLM (t_{llm}) for a given target fine-tuning dataset size.

The derivation starts with our two empirically fitted scaling law models for training time:

$$t_{ve} = k_v \cdot (r_{ve})^{\gamma_v} \cdot D_f^{\delta_v} + E_{ve} \quad (7)$$

$$t_{llm} = k_l \cdot (r_{llm})^{\gamma_l} \cdot D_f^{\delta_l} + E_{llm} \quad (8)$$

where $\Theta_{t_{ve}} = \{k_v, \gamma_v, \delta_v, E_{ve}\}$ and $\Theta_{t_{llm}} = \{k_l, \gamma_l, \delta_l, E_{llm}\}$ are the fitted coefficients.

To find the balance point, we set these two time estimates to be approximately equal ($t_{ve} \approx t_{llm}$) for a target dataset size, denoted as D_{target} . This gives the following relationship:

$$k_v \cdot (r_{ve})^{\gamma_v} \cdot D_{target}^{\delta_v} + E_{ve} \approx k_l \cdot (r_{llm})^{\gamma_l} \cdot D_{target}^{\delta_l} + E_{llm} \quad (9)$$

Our goal is to solve for r_{ve} . We begin by isolating the term containing r_{ve} on one side of the equation:

$$k_v \cdot (r_{ve})^{\gamma_v} \cdot D_{target}^{\delta_v} \approx k_l \cdot (r_{llm})^{\gamma_l} \cdot D_{target}^{\delta_l} + (E_{llm} - E_{ve}) \quad (10)$$

Finally, to solve for r_{ve} , we raise both sides to the power of $1/\gamma_v$, which yields the final expression¹:

$$r_{ve} \approx \left(\frac{k_l \cdot (r_{llm})^{\gamma_l} \cdot D_{target}^{\delta_l} + E_{llm} - E_{ve}}{k_v \cdot D_{target}^{\delta_v}} \right)^{\frac{1}{\gamma_v}} \quad (11)$$

H. Generality of MARS with Broader Benchmark Coverage

In Section 4.2, we evaluate MARS on broader benchmark suites, including generalist suites (MME, POPE, MMStar) and domain-specific tasks (GQA, TextCaps, AI2D), as provided by the *Multimodal Evaluation Toolkit* (Zhang et al., 2024c). Here, we provide a brief description of each benchmark along with the detailed numerical results omitted from Figure 3.

H.1. Benchmark Description

Table 6. Summary of Benchmarks and Evaluation Metrics

Benchmark	Focus	Metric in Figure 3
MME (Fu et al., 2023)	General perception and cognition	Cognition + Perception
POPE (Li et al., 2023)	Object hallucination	F1 Score
MMStar (Chen et al., 2024)	Visual perception and reasoning	Avg. Accuracy
GQA (Hudson & Manning, 2019)	Compositional visual reasoning	Accuracy
TextCaps (Sidorov et al., 2020)	OCT-based image captioning	ROUGE_L
AI2D (Kembhavi et al., 2016)	Scientific diagram understanding	Accuracy

H.2. Detailed Numbers for Figure 3

Table 7. Performance comparison on diverse multimodal benchmarks demonstrating the broad generalization of generalist models when MARS is applied to the connected VE and LLM

Method	MME (sum)	POPE	MMStar (avg)	TextCaps (Val)	AI2D	GQA
AdaLoRA (Zhang et al., 2023)	1524.0	79.7	28.6	38.0	45.5	52.7
LoRA (★, 64)	1662.4	86.8	36.1	42.6	48.0	55.1
MARS	1695.6	86.3	39.4	42.9	49.9	55.7

¹In very rare cases (0.72% of our total runs) where the numerator becomes non-positive, implying that E_{ve} is large due to the inherent entropy of the data distribution, we set $r_{ve} = r_{llm}$ to serve as a default LoRA configuration.

Table 8. Fine-grained capability breakdown on MMStar (Chen et al., 2024)

Method	Coarse Per.	Fine-Grained Per.	Instance Reason.	Logical Reason.	Sci & Tech	Math
AdaLoRA	34.7	23.2	27.8	29.9	24.4	31.5
LoRA (★, 64)	55.5	27.8	49.8	32.1	22.2	29.0
MARS	58.3	28.4	48.4	34.9	33.0	33.4

I. Simultaneous Multi-Rank Tuning for Scalability

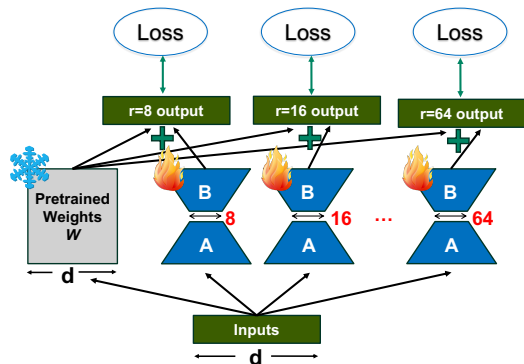


Figure 11. Simultaneous Multi-Rank Tuning Mechanism

Figure 11 illustrates our proposed optimization for the calibration phase, leveraging the frozen nature of the pre-trained backbone weights (W). In standard fine-tuning, the computationally expensive forward pass through the large backbone (W) must be recomputed for every distinct rank configuration tested. To eliminate this redundancy, we construct a computational graph where the backbone features are computed only once per batch. These shared features are then branched into multiple, lightweight parallel LoRA adapter heads (e.g., initialized with ranks $r = \{8, 16, 32, 64\}$). Since the LoRA parameters constitute a negligible fraction of the total model size ($< 1\%$), the computational overhead of running these parallel branches is minimal. This strategy allows us to gather perplexity and convergence statistics for all candidate ranks simultaneously in a single training run, in the best case, effectively reducing the calibration search cost from $\mathcal{O}(K^N)$ to $\mathcal{O}(1)$ (where K is the number of rank candidates and N is the number of modalities). This optimization ensures that MARS remains highly efficient even as the search space expands.